Organic Electronics 37 (2016) 465–473

Contents lists available at ScienceDirect

Organic Electronics

journal homepage: www.elsevier.com/locate/orgel

Panchromatic dyes having diketopyrrolopyrrole and ethylenedioxythiophene applied to dye-sensitized solar cells

Ichiro Imae*, Yohei Ito, Shun Matsuura, Yutaka Harima

Department of Applied Chemistry, Graduate School of Engineering, Hiroshima University, 1-4-1 Kagamiyama, Higashi-Hiroshima, Hiroshima 739-8527, Japan

ARTICLE INFO

Article history:
Received 10 June 2016
Received in revised form
12 July 2016
Accepted 18 July 2016

Keywords:
Dye-sensitized solar cells
Diketopyrrolopyrrole
Ethylenedioxythiophene
Panchromatic absorption

ABSTRACT

Novel panchromatic donor-acceptor-π-acceptor dyes (**DPP1**–**4**) containing diketopyrrolopyrrole (DPP) and 3,4-ethylenedioxythiophene (EDOT) have been designed and synthesized. Introduction of both DPP and EDOT units into a dye framework induced a remarkable red-shift of absorption bands and thus photoactive spectral regions of the dye-sensitized solar cells (DSSCs) based on the panchromatic **DPP1**–**4** dyes were extended far above 800 nm. Influences of alkyl substituents in **DPP1**–**4** on the performances of the DSSCs were discussed, and also those of co-adsorbate on TiO_2 and additive in the electrolyte used in the DSSC preparation were studied to optimize photovoltaic performances of the DSSCs.

1. Introduction

Since the first report of Grätzel et al., in 1991 [1,2], dye-sensitized solar cells (DSSCs) have attracted a considerable attention due to their high conversion efficiency of incident light to electricity and low production cost [3]. In order to improve the power conversion efficiency, many researchers have focused on the development of novel organic dyes [4–6]. Since donor-π-acceptor (D-π-A) dyes consisting of an electron donor (D) and an electron acceptor (A) linked through a π-conjugated bridge (π-linker) possess high molar absorption coefficients and their electronic properties can be easily tuned by molecular modifications, many types of D-π-A dyes have been enthusiastically synthesized [7–11]. In 2010, Tian et al. reported a new concept of a donor-acceptor-π-acceptor (D-A-π-A) structure for designing a new generation of efficient dye-sensitizers [12]. In this D-A-π-A structure, an additional electron-acceptor unit such as diketopyrrolopyrrole (DPP), benzothiadiazole, benzotriazole, and quinoxaline has been introduced into the π-linker of the D-π-A framework, so that the absorption spectral response has been extended to the near infrared region [13,14]. DPP was originally developed as a commercially available industrial pigment for the application to car-paint pigments and polymeric organic photovoltaics [15–17], and is expected to have a strong light-harvesting ability. From this viewpoint, several DPP-containing D-A-π-A dyes have been synthesized [12,15,18–30].

We have recently developed novel D-π-A dyes containing 3,4-ethylenedioxythiophene (EDOT) in the oligothiophenes as π-linkers [31,32]. These D-π-A dyes demonstrated a successful expansion of spectral response due to a remarkable red-shift of absorption bands caused by introduction of EDOT [33–37]. In our present study, a novel class of D-A-π-A dyes having both DPP and EDOT units (**DPP1**–**4**) have been designed and synthesized (Fig. 1), in order to further improve the light-harvesting ability of the D-π-A dyes by utilizing both characteristics of DPP and EDOT. The performances of DSSCs based on the D-A-π-A dyes are discussed in comparison with those for **PE4T**, which has an EDOT-containing quaterthiophene as a π-linker with no DPP unit [31], and for **MK-2** known well as a D-π-A dye having oligothiophene for the high-performance DSSC [38].

2. Experimental

2.1. Materials

n-Hexane, toluene, tetrahydrofuran (THF), *N*,*N*-dimethylformamide (DMF), acetic acid (AcOH), chloroform ($CHCl_3$),

* Corresponding author.
E-mail address: imae@hiroshima-u.ac.jp (I. Imae).

http://dx.doi.org/10.1016/j.orgel.2016.07.022
1566-1199/

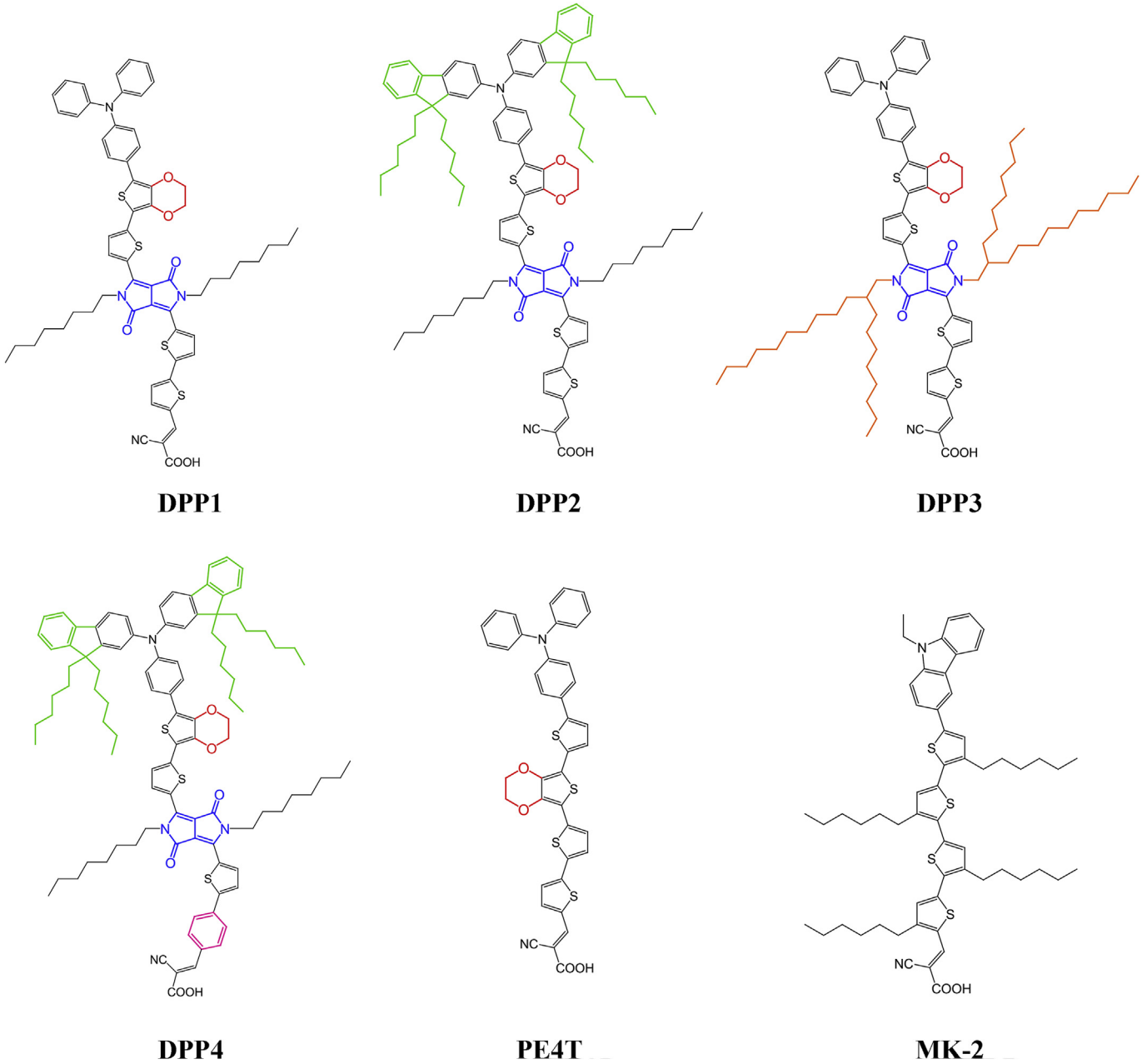

Fig. 1. Chemical structures of **DPP1**–**4**, **PE4T**, and **MK-2**.

dichloromethane (CH_2Cl_2), methanol (MeOH), and acetonitrile were purified by standard methods and used immediately after purification. Tetrabutylammonium perchlorate (TBAP) and *N*-bromosuccinimide (NBS) were purified by recrystallization from ethanol and benzene, respectively, and dried under vacuum. EDOT, 5-formyl-2-thiopheneboronic acid (**7a**), 4-formylphenylboronic acid (**7b**), and cyanoacetic acid (**9**) were purchased from Tokyo Chemical Industry and used without further purification. Tetrakis(triphenylphosphine)palladium (0) ($Pd(PPh_3)_4$) purchased from Kanto Chemical was used as the catalyst of the Stille and Suzuki reactions. 5-(2-Carboxy-2-cyanovinyl)-[5‴-(9-ethyl-9*H*-carbazol-3-yl)-3′,3″,3‴,4-tetra-*n*-hexyl-2,2′:5′,2″:5″,2‴-quaterthiophene (**MK-2**) was purchased from Aldrich.

2.2. Synthesis

The synthetic routes of D-A-π-A dyes having both EDOT and DPP units are shown in Scheme 1. The starting compounds, *N*-(4-bromophenyl)-*N*,*N*-diphenylamine (**1a**) [39], *N*,*N*-bis(9,9-dihexyl-9*H*-fluoren-2-yl)-*N*-(4-bromophenyl)amine (**1b**) [40], 2-tributylstannyl-3,4-ethylenedioxythiophene (**2**) [35], and 3,6-bis(5-bromo-2-thienyl)-2,5-dialkyl-2,5-dihydropyrrolo[3,4-*c*]pyrrole-1,4-dione (**5**) [41] were synthesized according to previously published procedures. The Stille coupling reaction of bromotriarylamine (**1**) and stannyl-EDOT (**2**) gave the compounds **3**. Compounds **4** were obtained by a reaction between tributyltin-chloride with an organolithium compound obtained from **3** and *n*-BuLi, and were used for the Stille reaction with bis(bromothienyl)-DPP (**5**) to give the compounds **6**. Suzuki coupling reaction between

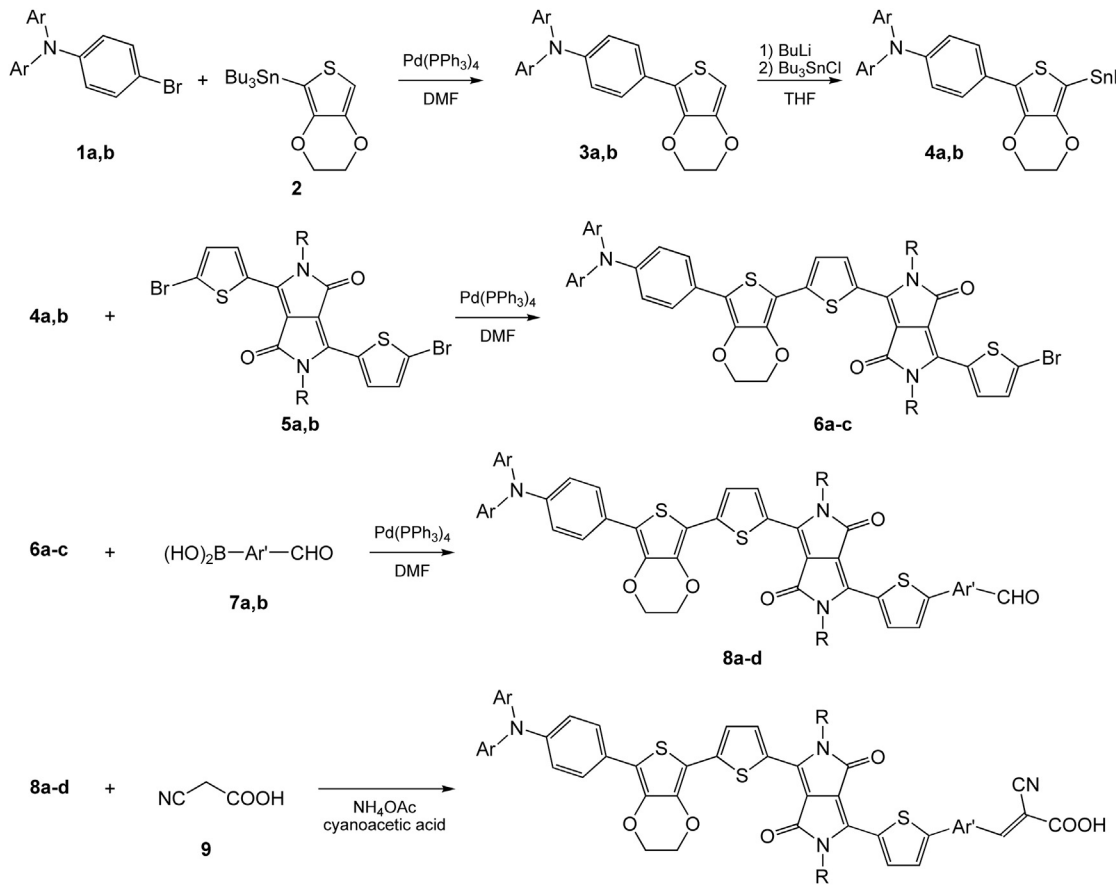

Scheme 1. Synthetic routes of **DPP1**–**4**.

6 and formylaryl boronic acid (**7**) gave the compounds **8**, which were converted to the corresponding sensitizing dyes by Knoevenagel condensation with cyanoacetic acid (**9**). Detailed synthetic processes for some intermediate chemicals and target dyes and their characterizations are described below.

2.2.1. 2-[4-(N,N-Diphenylamino)phenyl]-3,4-ethylenedioxythiophene (**3a**, Ar = phenyl)

Under a nitrogen atmosphere, a mixture of **1a** (1.1 g, 3.4 mmol), **2** as-prepared from EDOT (0.73 g, 5.6 mmol), and $Pd(PPh_3)_4$ (0.47 g, 0.44 mmol) were dissolved in DMF (10 mL). The resulting solution was stirred at 80 °C for 12 h. The mixture was poured into water and then extracted with CH_2Cl_2. The organic extract was dried over Na_2SO_4. After removal of the solvent, the residue was purified by a column chromatography (silica gel, *n*-hexane/CH_2Cl_2 (1/2)). Compound **3a** (0.47 g, 1.2 mmol) was obtained as a pale yellow liquid. Yield: 36%. ^{1}H NMR (500 MHz, CD_2Cl_2, δ, ppm): 4.21–4.31 (m, 4H, OC***H***$_2$C***H***$_2$O), 6.25 (s, 1H, thienyl-***H***), 7.00–7.05 (m, 2H, phenyl-***H***), 7.03 (d, J = 8.83 Hz, 2H, phenylene-***H***), 7.06–7.11 (m, 4H, phenyl-***H***), 7.23–7.29 (m, 4H, phenyl-***H***), 7.57 (d, J = 8.83 Hz, 2H, phenylene-***H***).

2.2.2. 2-[4-(N,N-Diphenylamino)phenyl]-5-tributylstannyl-3,4-ethylenedioxythiophene (**4a**, Ar = phenyl)

To a THF (15 mL) solution of **3a** (0.47 g, 1.2 mmol), 0.74 mL of *n*-butyl lithium (1.65 M in *n*-hexane, 1.2 mmol) was added at −78 °C. After 1 h, tributyltin chloride (0.40 g, 1.2 mmol) was added in one portion. The reaction mixture was stirred at −78 °C for 30 min and then at room temperature for 1 h. After the solvent was removed using a rotary evaporator, *n*-hexane was added and the solution was stirred for 1 h. After filtration of the solution, the solvent was removed using a rotary evaporator. A yellow liquid was obtained upon solvent removal. Product was used without further purification.

2.2.3. 3-(5-Bromo-2-thienyl)-6-{5′-[4-(N,N-diphenylamino)phenyl]-3′,4′-ethylenedioxy-2,2′-bithien-5-yl}-2,5-di(n-octyl)-2,5-dihydropyrrolo[3,4-c]pyrrole-1,4-dione (**6a**, Ar = phenyl, R = n-octyl)

Under a nitrogen atmosphere, a mixture of **4a** obtained from **3a** (0.47 g, 1.2 mmol), **5a** (0.83 g, 1.2 mmol), and $Pd(PPh_3)_4$ (0.14 g, 0.13 mmol) were dissolved in toluene (20 mL). The resulting solution was stirred at 80 °C for 12 h. The mixture was poured into water and then extracted with $CHCl_3$. The organic extract was dried over Na_2SO_4. After removal of the solvent, the residue was purified by a column chromatography (silica gel, toluene). Compound **6a** (60 mg, 61 μmol) was obtained as a purple solid. Yield: 6%. ^{1}H NMR (500 MHz, CD_2Cl_2, δ, ppm): 0.86 (t, J = 7.14 Hz, 3H, C***H***$_3$), 0.88 (t, J = 7.14 Hz, 3H, C***H***$_3$), 1.22–1.48 (m, 20H, (C***H***$_2$)$_5$CH$_3$), 1.62–1.81 (m, 4H, *N*-CH$_2$C***H***$_2$), 3.98 (t, J = 7.80 Hz, 2H, *N*-C***H***$_2$), 4.07 (t, J = 7.80 Hz, 2H, *N*-C***H***$_2$), 4.34–4.50 (m, 4H, OC***H***$_2$C***H***$_2$O), 7.04 (d, J = 8.80 Hz, 2H,

phenylene-***H***), 7.03–7.08 (m, 2H, phenyl-***H***), 7.08–7.13 (m, 4H, phenyl-***H***), 7.24 (d, $J = 4.26$ Hz, 1H, thienylene-***H***), 7.25–7.31 (m, 4H, phenyl-***H***), 7.36 (br, 1H, thienylene-***H***), 7.60 (d, $J = 8.80$ Hz, 2H, phenylene-***H***), 8.61 (br, 1H, thienylene-***H***), 9.05 (d, $J = 3.91$ Hz, 1H, thienylene-***H***).

2.2.4. 3-(5′-Formyl-2,2′-bithien-5-yl)-6-{5′-[4-(N,N-diphenylamino)phenyl]-3′,4′-ethylenedioxy-2,2′-bithien-5-yl}-2,5-di(n-octyl)-2,5-dihydropyrrolo[3,4-c]pyrrole-1,4-dione (8a, Ar = phenyl, R = n-octyl, Ar′ = 2,5-thienylene)

Under a nitrogen atmosphere, a mixture of **6a** (56 mg, 57 μmol), **7a** (15 mg, 0.60 mmol), and $Pd(PPh_3)_4$ (10 mg, 9.5 μmol) was dissolved in THF (9 mL). To this solution, Na_2CO_3 (16 mg, 0.15 mmol) in water (3 mL) was added. The resulting solution was stirred at 80 °C for 16 h. The mixture was poured into water and then extracted with $CHCl_3$. The organic extract was dried over Na_2SO_4. After removal of the solvent, the residue was washed by acetone. Compound **8a** (30 mg, 29 μmol) was obtained as a reddish purple solid. Yield: 52%. ^{1}H NMR (500 MHz, CD_2Cl_2, δ, ppm): 0.86 (t, $J = 6.88$ Hz, 3H, C***H***$_3$), 0.87 (t, $J = 6.88$ Hz, 3H, C***H***$_3$), 1.24–1.41 (m, 20H, (C***H***$_2$)$_5$CH$_3$), 1.71–1.81 (m, 4H, *N*-CH$_2$C***H***$_2$), 4.07 (t, $J = 8.72$ Hz, 2H, *N*-C***H***$_2$), 4.09 (t, $J = 8.72$ Hz, 2H, *N*-C***H***$_2$), 4.35–4.48 (m, 4H, OC***H***$_2$C***H***$_2$O), 7.03 (d, $J = 8.80$ Hz, 2H, phenylene-***H***), 7.04–7.08 (m, 2H, phenyl-***H***), 7.08–7.12 (m, 4H, phenyl-***H***), 7.25–7.31 (m, 4H, phenyl-***H***), 7.36 (d, $J = 4.34$ Hz, 1H, thienylene-***H***), 7.39 (d, $J = 3.97$ Hz, 1H, thienylene-***H***), 7.49 (d, $J = 4.16$ Hz, 1H, thienylene-***H***), 7.60 (d, $J = 8.80$ Hz, 2H, phenylene-***H***), 7.71 (d, $J = 3.97$ Hz, 1H, thienylene-***H***), 8.88 (d, $J = 4.16$ Hz, 1H, thienylene-***H***), 9.09 (d, $J = 4.34$ Hz, 1H, thienylene-***H***), 9.86 (s, 1H, C***H***O).

2.2.5. 3-[5′-(2-Carboxy-2-cyanovinyl)-2,2′-bithien-5-yl]-6-{5′-[4-(N,N-diphenylamino)phenyl]-3′,4′-ethylenedioxy-2,2′-bithien-5-yl}-2,5-di(n-octyl)-2,5-dihydropyrrolo[3,4-c]pyrrole-1,4-dione (DPP1, Ar = phenyl, R = n-octyl, Ar′ = 2,5-thienylene)

A mixture of **8a** (30 mg, 30 μmol), **9** (25 mg, 0.30 mmol) and ammonium acetate (2.3 mg, 0.029 mmol) in acetic acid (2 mL) was refluxed for 16 h under a nitrogen atmosphere. The mixture was cooled down to room temperature and the solvent was evaporated under reduced pressure. The crude product was washed with acetic acid (20 mL) and diethylether/*n*-hexane (1/1) (40 mL) in this order. **DPP1** (17 mg, 16 μmol) was obtained as a dark-green solid. Yield: 52%. ^{1}H NMR (500 MHz, acetone-d$_6$, δ, ppm): 0.82 (t, $J = 7.25$ Hz, 6H, C***H***$_3$), 1.05–1.22 (m, 20H, (C***H***$_2$)$_5$CH$_3$), 1.78–1.82 (m, 4H, *N*-CH$_2$C***H***$_2$), 4.12–4.18 (br, 4H, *N*-C***H***$_2$), 4.46–4.63 (m, 4H, OC***H***$_2$C***H***$_2$O), 5.62 (s, 1H, vinylene-***H***), 7.06–7.78 (m, 18H, Ar-***H***), 8.98 (d, $J = 3.94$ Hz, 1H, thienylene-***H***), 9.19 (d, $J = 3.94$ Hz, 1H, thienylene-***H***). HRMS (ESI) m/z calcd for $C_{62}H_{60}O_6N_4S_4$ 1084.33902 (M^+), found 1084.33809 (M^+).

2.2.6. 3-[5′-(2-Carboxy-2-cyanovinyl)-2,2′-bithien-5-yl]-6-(5′-{4-[N,N-bis(9,9-dihexyl-9H-fluoren-2-yl)amino]phenyl}-3′,4′-ethylenedioxy-2,2′-bithien-5-yl)-2,5-di(n-octyl)-2,5-dihydropyrrolo[3,4-c]pyrrole-1,4-dione (DPP2, Ar = 9,9-dihexyl-9H-fluoren-2-yl, R = n-octyl, Ar′ = 2,5-thienylene)

DPP2 was prepared according to the same procedure as described for **DPP1** by using *N*,*N*-bis(9,9-dihexyl-9*H*-fluoren-2-yl)-4-bromoaniline as a starting material. ^{1}H NMR (500 MHz, acetone-d$_6$, δ, ppm): 0.76–0.94 (m, 18H, C***H***$_3$), 1.04–1.24 (m, 52H, methylene-***H***), 1.78–1.86 (m, 4H, *N*-CH$_2$C***H***$_2$), 1.94–2.00 (m, 8H, fluorene-C***H***$_2$), 4.10–4.20 (br, 4H, *N*-C***H***$_2$), 4.45–4.62 (m, 4H, OC***H***$_2$C***H***$_2$O), 5.62 (s, 1H, vinylene-***H***), 7.06–7.80 (m, 22H, Ar-***H***), 8.98 (d, $J = 3.86$ Hz, 1H, thienylene-***H***), 9.19 (d, $J = 3.86$ Hz, 1H, thienylene-***H***). HRMS (ESI) m/z calcd for $C_{100}H_{117}O_6N_4S_4$ 1597.78505 ([M+H]$^+$), found 1597.78198 ([M+H]$^+$).

2.2.7. 3-[5′-(2-Carboxy-2-cyanovinyl)-2,2′-bithien-5-yl]-6-{5′-[4-(N,N-diphenylamino)phenyl]-3′,4′-ethylenedioxy-2,2′-bithien-5-yl}-2,5-di(2-octyldodecyl)-2,5-dihydropyrrolo[3,4-c]pyrrole-1,4-dione (DPP3, Ar = phenyl, R = 2-octyldodecyl, Ar′ = 2,5-thienylene)

DPP3 was prepared according to the same procedure as described for **DPP1** by using 3,6-bis(5-bromo-2-thienyl)-2,5-di (2-octyldodecyl)-2,5-dihydropyrrolo [3,4-*c*]pyrrole-1,4-dione as a starting material. ^{1}H NMR (500 MHz, acetone-d$_6$, δ, ppm): 0.78–0.88 (m, 12H, C***H***$_3$), 1.10–1.50 (m, 64H, methylene-***H***), 1.98–2.03 (m, 2H, *N*-CH$_2$C***H***), 3.98–4.08 (br, 4H, *N*-C***H***$_2$), 4.40–4.60 (m, 4H, OC***H***$_2$C***H***$_2$O), 5.57 (s, 1H, vinylene-***H***), 7.04–7.74 (m, 18H, Ar-***H***), 9.01 (d, $J = 4.12$ Hz, 1H, thienylene-***H***), 9.19 (d, $J = 4.12$ Hz, 1H, thienylene-***H***). HRMS (ESI) m/z calcd for $C_{86}H_{108}O_6N_4S_4$ 1420.71462 (M^+), found 1420.71375 (M^+).

2.2.8. 3-{5-[4-(2-Carboxy-2-cyanovinyl)phenyl]-2-thienyl}-6-(5′-{4-[N,N-bis(9,9-dihexyl-9H-fluoren-2-yl)amino]phenyl}-3′,4′-ethylenedioxy-2,2′-bithien-5-yl)-2,5-di(n-octyl)-2,5-dihydropyrrolo[3,4-c]pyrrole-1,4-dione (DPP4, Ar = 9,9-dihexyl-9H-fluoren-2-yl, R = n-octyl, Ar′ = 1,4-phenylene)

DPP4 was prepared according to the same procedure as described for **DPP2** by using 4-formylphenylboronic acid for the synthesis of compound **8**.^{1}H NMR (500 MHz, DMSO-d$_6$, δ, ppm): 0.70–0.92 (m, 18H, C***H***$_3$), 0.94–1.16 (m, 52H, methylene-***H***), 1.58–1.72 (m, 4H, *N*-CH$_2$C***H***$_2$), 1.80–1.94 (m, 8H, fluorene-C***H***$_2$), 3.96–4.07 (br, 4H, *N*-C***H***$_2$), 4.32–4.54 (m, 4H, OC***H***$_2$C***H***$_2$O), 5.75–5.78 (br, 1H, vinylene-***H***), 6.92–8.02 (m, 24H, Ar-***H***), 8.76–8.81 (br, 1H, thienylene-***H***), 8.98–9.01 (br, 1H, thienylene-***H***). HRMS (ESI) m/z calcd for $C_{102}H_{118}O_6N_4S_3$ 1590.82080 (M^+), found 1590.81983 (M^+).

2.3. Characterizations

^{1}H NMR spectra were recorded by a 500 MHz spectrometer (Varian Inc., NMR System 500). Measurements of mass spectroscopies were made using a GC-TOFMS (gas chromatograph—time-of-flight mass spectrometry, JEOL, JMS-T100GCV (AccuTOF GCv 4G)) and an ESI-FTMS (electron spray Fourier transformed mass spectrometry, Thermo Fisher Scientific, LTQ Orbitrap XL). UV–vis absorption and fluorescence spectra were taken on a Shimadzu UV-3150 spectrophotometer and a Hitachi F-4500 fluorescence spectrophotometer, respectively. Cyclic voltammetry (CV) was carried out with a potentiostat/galvanostat (Hokuto Denko, HZ-3000) using a three-electrode system with a Pt working electrode, a Pt wire counter electrode, and a Ag/Ag$^+$ reference electrode. The supporting electrolyte was 0.1 M TBAP in dichloromethane. The potential of the reference electrode was calibrated by ferrocene after each set of measurements. Potentials referred to ferrocene were then converted to the Normal Hydrogen Electrode (NHE) standard by addition of 0.63 V [42].

2.4. Fabrication of DSSCs and photovoltaic measurements

The TiO_2 paste (JGC Catalysts and Chemicals Ltd., PST-18NR) was deposited on a fluorine-doped-tin-oxide (FTO) substrate by doctor-blading and sintered for 50 min at 450 °C. The 9 μm thick TiO_2 electrode (0.5 × 0.5 cm^2 in a photoactive area) was immersed into a 0.1 mM dye solution of CH_2Cl_2/MeOH (10/1, v/v) for adsorption of the photosensitizer. The DSSCs were fabricated using the dye-adsorbed TiO_2 electrode, Pt-coated glass as a counter electrode, and a solution of 0.05 M iodine, 0.1 M lithium iodide, and 0.6 M 1,2-dimethyl-3-propylimidazolium iodide (DMPrII) in acetonitrile as the electrolyte. The photocurrent (*J*)-voltage (*V*) characteristics were measured using a potentiostat under a simulated solar light (AM 1.5, 100 mW cm^{-2}) supplied by a solar simulator (Asahi Spectra

HAL-302). The incident photon-to-current conversion efficiency (IPCE) spectra were measured under monochromatic irradiation using a tungsten-halogen lamp (Shimadzu AT-100HG) and a monochromator (Shimadzu SPG-120 S).

2.5. Estimation of amount of dye molecules adsorbed on TiO_2

A specific surface area of the sintered TiO_2 powder was determined by nitrogen adsorption experiments at 77 K. When the temperature of the TiO_2 electrode was cooled to 40 °C, the sintered electrode was immersed into CH_2Cl_2/MeOH (10/1, v/v) solutions containing various concentrations of the DPP dyes for adsorption of the dyes. In all cases, the dye adsorption was performed for 18 h at room temperature. The dye-adsorbed TiO_2 electrode was cautiously soaked in pure CH_2Cl_2/MeOH (10/1, v/v) for several seconds to remove a trace of dying solution from the void of nanoporous TiO_2 electrode. Subsequently, dye molecules adsorbed on TiO_2 were desorbed in a mixed solution (CH_2Cl_2/MeOH/Bu_4NOH (37% in MeOH) 10/0.9/0.1, v/v/v) and the absorption spectra of the solutions were measured to determine the amount of adsorption of the DPP dyes on the TiO_2 surface.

3. Results and discussion

Density functional theory (DFT) calculations were performed using a Gaussian 09 software at the Becke three-parameter hybrid functional combined with Lee–Yang–Parr correlation functional (B3LYP) with a polarized 6-31G(d) basis set [43]. The theoretically calculated energy levels and electronic-density distribution of **DPP1** are shown in Fig. 2. The calculation results demonstrated that the electronic density of the HOMO of **DPP1** was delocalized from the triarylamine (TArA) to DPP unit, whereas that of the LUMO was delocalized from DPP unit to cyanoacrylic acid (CA), indicating that an intramolecular charge transfer (ICT) can occur from the TArA group to the CA unit upon illumination. Electron densities of HOMOs and LUMOs of other DPP-dyes were similar to those of **DPP1**, indicating that the introduction of fluorene and bulky alkyl chains did not affect their electronic structures considerably. It was found that four alkyl groups introduced in fluorene and DPP units of **DPP2** and **DPP3**, respectively, were perpendicularly located to the π-plane of fluorene and DPP units (Fig. S1, see supporting information).

Optical absorption and fluorescence spectra of **DPP1**–**4** and **PE4T** in dichloromethane are shown in Fig. 3 and their spectral data are summarized in Table 1. **DPP1**–**4** exhibited two major absorption bands at ca. 400 nm and ca. 650 nm, where the former band is attributed to the π-π* transition and the latter is assigned to the ICT from TArA to CA unit. Compared with **DPP1**, the introduction of bulky groups on TArA (**DPP2**) and DPP (**DPP3**) did not change the light-absorption wavelength regions, but enhanced the molar absorption coefficients (εs). On the other hand, the replacement of a thiophene ring placed between DPP and CA units with a benzene ring (**DPP4**) caused the blue-shift of absorption bands. We note also that the ICT bands of **DPP1**–**4** (650 nm) are located at wavelengths longer than that of **PE4T** (500 nm). This demonstrates that the introduction of an additional electron acceptor of DPP into the D-π-A framework induced a remarkable red-shift of the ICT band by 200 nm due to a strong accepting ability of the DPP unit. Absorption band edges of the D-A-π-A dyes (**DPP1**–**4**) developed in this study were extended beyond 800 nm compared with those of 700 nm or below for most of DPP-dyes reported earlier [12,18–30]. The band-edge extinction due to the introduction of EDOT unit in π-linkers is responsible, in part, for the panchromatic nature of **DPP1**–**4**.of **DPP1**–**4** and **PE4T** in dichloromethane.

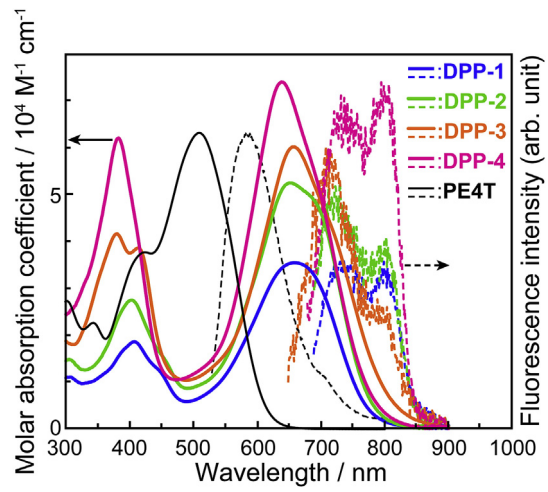

Fig. 3. Optical absorption (solid line) and fluorescence (dashed line) spectra.

Cyclic voltammetry (CV) was conducted to evaluate the feasibility of electron injection and the possibility of dye regeneration for **DPP1**–**4** developed in this study. Fig. 4 displays the CV curves of **DPP1**–**4** in dichloromethane, measured with an initial anodic scan of potential from −0.5 V vs. Fc/Fc^+. The HOMO energy levels of **DPP1**–**4** evaluated from the half-wave potential ($E_{1/2}^{OX}$) for the first redox step were 0.84, 0.81, 0.86, and 0.77 V, slightly less positive than 0.89 V *vs.* NHE for **PE4T**. The LUMO energy levels were calculated to be −0.93, −0.96, −0.91, and −1.00 V from the HOMO energy and the bandgap energy ($E_{0\text{-}0}$) estimated from the intersection of the normalized absorption and fluorescence spectra. These energy levels of **DPP1**–**4** and **PE4T** are summarized in Table 1 and they are illustrated also in Fig. S2, along with the positions of the conduction band edge (E_{CB}) of TiO_2 (−0.5 V *vs.* NHE) and the

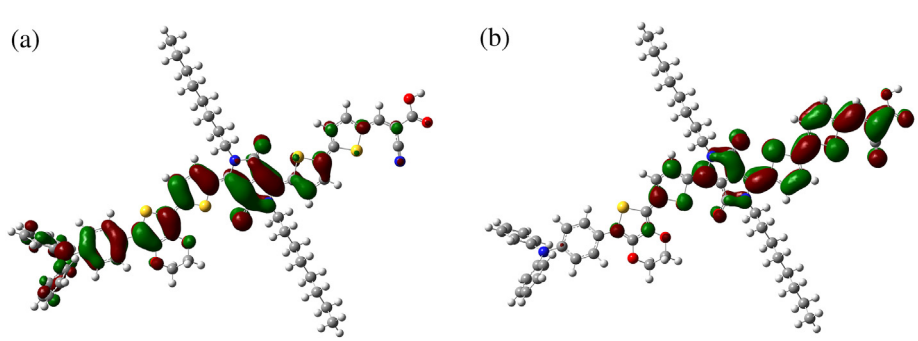

Fig. 2. Frontier molecular orbitals optimized by Gaussian 09 at B3LYP/6-31G(d) level for (a) HOMO and (b) LUMO of **DPP1**.

Table 1
Optical and electrochemical properties of **DPP1–4** and **PE4T**.

Dye	Absorption[a]		Fluorescence[a]	Energy levels/V *vs.* NHE		
	λ_{max}/nm	$10^{-4}\ \varepsilon_{max}/M^{-1}\ cm^{-1}$	λ_{max}/nm	E_{HOMO}[b]	$E_{0\text{-}0}$[c]	E_{LUMO}[d]
DPP1	658/408	3.56/1.88	724	0.84	1.75	−0.93
DPP2	651/405	5.27/2.77	727	0.81	1.77	−0.96
DPP3	656/381	6.04/4.18	724	0.86	1.77	−0.91
DPP4	638/383	7.42/6.23	727	0.77	1.77	−1.00
PE4T[e]	510/425	6.33/3.78	590	0.89	2.22	−1.33

[a] Absorption and fluorescence spectra were recorded in dichloromethane.
[b] Determined by cyclic voltammetry.
[c] Determined from the intersection of absorption and emission spectra.
[d] Calculated from $E_{HOMO} - E_{0\text{-}0}$.
[e] Data from Ref. [31].

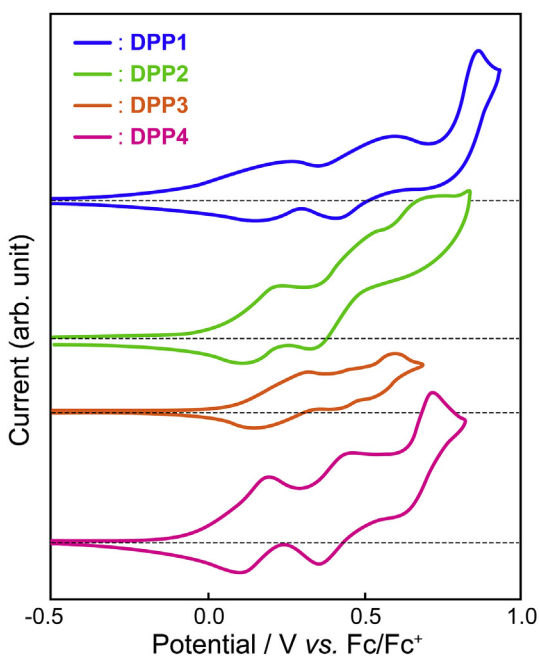

Fig. 4. Cyclic voltammograms of **DPP1–4** (1 mM) in dichloromethane containing TBAP (0.1 M) at a scan rate of 50 mV s^{-1}.

Fermi level energy of the I^-/I_3^- redox couple (*ca.* 0.4 V vs. NHE). It is seen from Fig. S2 that the HOMO and LUMO levels are similar for **DPP1–3**, whereas both energy levels of **DPP4** in which a thiophene ring placed between DPP and CA units in **DPP2** is replaced with a benzene ring are shifted slightly upward relative to those of **DPP1–3**. On the other hand, the LUMO levels of **DPP1–4** (−0.91 to −1.00 V) lie below that of **PE4T** (−1.33 V) due to the introduction of the strong electron-accepting DPP unit into **PE4T**. The estimated HOMO levels of all the dyes are located well above the E_{CB} of TiO_2 and the LUMO levels are below the Fermi level of the redox couple. These results indicate that an electron injection from the photo-excited sensitizer into the conduction band of TiO_2 and a regeneration of the oxidized dye by iodide in the electrolyte are feasible in the DSSCs based on **DPP1–4** and **PE4T**.

In order to investigate the steric effects of the alkyl substituents on TArA and DPP units in the DPP dyes, the amounts of dyes adsorbed on the nanocrystalline TiO_2 surface were measured as a function of the dye concentration for **DPP1–3**. Fig. 5 depicts adsorption isotherms for the three dyes in a double-logarithmic representation. The amount of adsorbed dyes (C_{ad}) on the ordinate is expressed by the number of dye molecules per unit area of the TiO_2 surface calculated using a specific surface area of 83 $m^2\ g^{-1}$

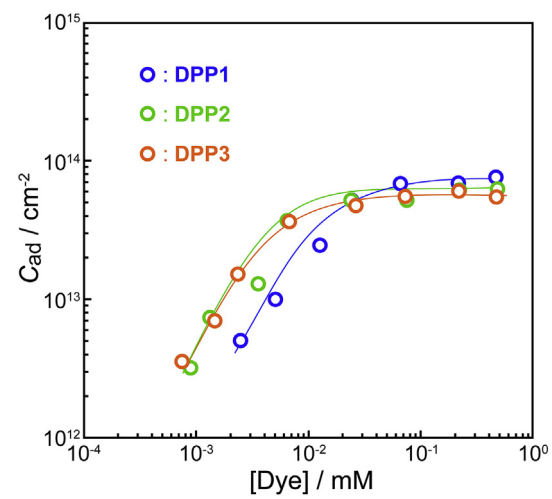

Fig. 5. Adsorption isotherms of **DPP1–3** on nanoporous TiO_2 electrodes.

for PST-18NR [44]. The abscissa denotes concentrations of dyes in equilibrium with dye-adsorbed TiO_2 electrodes in CH_2Cl_2/MeOH (10/1, v/v). These adsorption isotherms were analyzed on the basis of the following equation:

$$C_{ad}^{-1} = (K\ C_0)^{-1}[\mathrm{Dye}]^{-1} + C_0^{-1} \quad (1)$$

derived from a Langmuir isotherm [45–51].

$$C_{ad}/C_0 = K[\mathrm{Dye}]/(1 + K[\mathrm{Dye}]) \quad (2)$$

where C_{ad}, C_0, K, and [Dye] denote the amount of adsorbed dye, adsorbed amount at saturation, adsorption equilibrium constant, and equilibrium concentration of dye in solution, respectively. Fig. 6 represents plots of C_{ad}^{-1} against $[\mathrm{Dye}]^{-1}$ obtained from the data of Fig. 5. The plots fit straight lines well, demonstrating that adsorptions of these dyes on TiO_2 surfaces follow a Langmuir isotherm. The amounts of dyes adsorbed at saturation, C_0s, which can be estimated from the intercepts of these lines, were found to be 13.2×10^{13}, 8.2×10^{13} and $6.8 \times 10^{13}\ cm^{-2}$ for **DPP1–3**, respectively (Table 2). We have already found that the density of Brønsted-acid sites on which of TiO_2 surface organic dyes with carboxyl anchor are adsorbed is around $1.5 \times 10^{14}\ cm^{-2}$ for PST-18NR [44]. This value is comparable to the C_o value of **DPP1**, suggesting that **DPP1** molecules are almost fully adsorbed on available Brønsted-acid sites of TiO_2 surface. On the other hands, the decreased C_0 values for **DPP2** and **DPP3** are indicative of the increased bulkiness of alkyl groups introduced into the two dyes. Although C_0 value of **DPP4** was not estimated, it will be similar to that of **DPP2**. These results

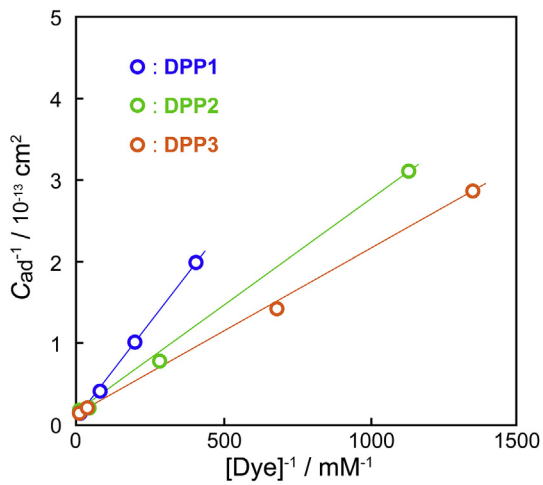

Fig. 6. Double-reciprocal plots for the data shown in Fig. 6. Fitting lines were obtained from the linear-least-squares method.

Table 2
Adsorption parameters of **DPP1**–**3** obtained from Langmuir isotherms.

Dye	C_0/cm^{-2}	K/mM^{-1}
DPP1	13.2×10^{13}	16.2
DPP2	8.2×10^{13}	46.2
DPP3	6.8×10^{13}	74.4

suggest that the introduction of bulky substituents in TArA or DPP units decreases the C_0s and will suppress the interaction between dye molecules on TiO_2.

Fig. 7 depicts the IPCE spectra and $J-V$ curves of DSSCs based on **DPP1**–**4** and **PE4T**, where any additives such as chenodeoxycholic acid (CDCA) and *tert*-butyl pyridine (TBP) used conventionally for optimizing DSSC performances [52–54] were not employed in order to get an insight into essential natures of the respective dyes used in the DSSCs as photosensitizers. Detailed photovoltaic parameters are listed in Table 3, together with those for DSSCs prepared using co-adsorbate on TiO_2 (CDCA) and/or additive to the electrolyte (TBP). Photovoltaic performances for a typical organic dye, **MK-2**, are also included in Table 3 for a reference. It is seen clearly from the IPCE spectra of Fig. 7(a) that the photoactive spectral regions of the DSSCs based on **DPP1**–**4** are extended far above 800 nm with extremely broad peaks centered at 600 nm in comparison with that for **PE4T** which has no DPP unit in the dye framework, demonstrating that we are successful in the preparation of panchromatic dyes for DSSCs. Fig. 7(b) shows that the J_{sc} values of the DSSCs prepared with **DPP1**–**4** are greater than that for **PE4T**. This can be ascribed to the enhanced spectral response of the DSSCs based on the panchromatic **DPP1**–**4** dyes. We note also in Fig. 7(b) that the J_{sc} values are increased systematically on the order of **DPP1**–**4**. According to the adsorption study of **DPP1**–**3** on TiO_2 described above, the maximum adsorbed amounts of these dyes (C_0 values) are decreased from **DPP1** to **DPP3**, corresponding to the order of the sizes of alkyl substituents introduced. In view of this, the increased J_{sc} values from **DPP1** to **DPP3** are likely to be attributed, at least in part, to the suppression of dye aggregation due to the increased steric hindrance of the bulky substituents. On the other hand, **DPP4** in which one of thiophene rings of **DPP2** is replaced with a benzene ring gives the largest J_{sc} value among DSSCs based on **DPP1**–**4**. Since the sizes of the two dye molecules are similar with each other, the dye aggregation cannot be responsible for a proper reason for the difference in J_{sc} between

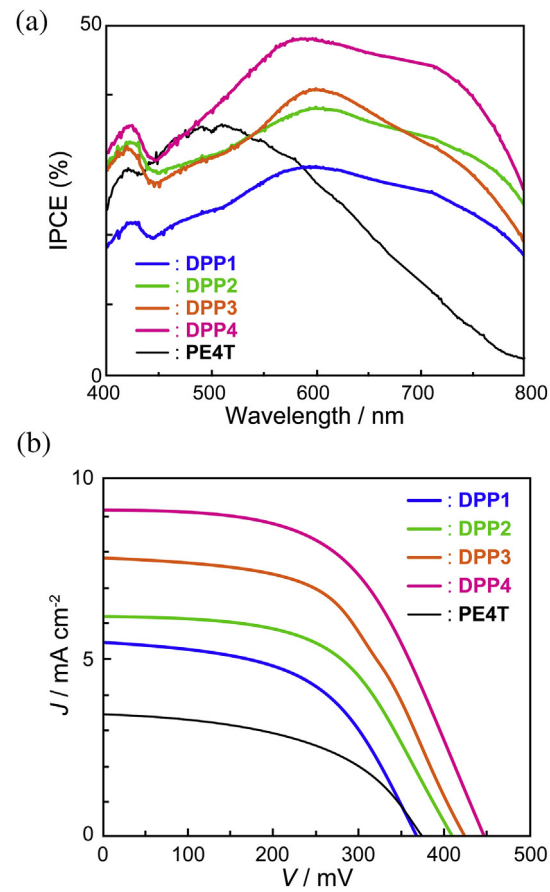

Fig. 7. (a) IPCE spectra and (b) $J-V$ characteristics of DSSCs based on **DPP1**–**4** and **PE4T**.

DPP2 and **DPP4**. Based on the energy schemes of **DPP2** and **DPP4** illustrated in Fig. S2, we presume that the upward shift of the LUMO level of **DPP4** relative to that of **DPP2**, induced by the replacement of thiophene with benzene, leads to the enhanced probability of an electron injection from LUMO to the conduction band of TiO_2 and thus results in the J_{sc} value of **DPP4** larger than that of **DPP2**.

In order to optimize photovoltaic performances of the DSSCs based on **DPP1**–**4** as well as to get a deeper insight into these panchromatic dyes, possible influences of the co-adsorption of CDCA on TiO_2 and/or the addition of TBP into the redox electrolyte were examined. At first, we will discuss influences of CDCA on the photovoltaic performances. The experiments were made with different concentrations of CDCA added in the dye solution and only the results which gave the best performances are listed in Table 3. We note that the addition of CDCA enhanced the η values for all the DSSCs: 1.1–2.1% for **DPP1**, 1.4–2.1% for **DPP2**, 1.8–2.0% for **DPP3**, and 2.2–3.3% for **DPP4**. As is seen from Table 3, the principal reason for the enhanced η values is ascribable to the increase of J_{sc}: 5.4–8.8 mA cm^{-2} for **DPP1**, 6.2–9.0 mA cm^{-2} for **DPP2**, 7.8–8.9 mA cm^{-2} for **DPP3**, and 9.2–13.7 mA cm^{-2} for **DPP4**. It is interesting to note in Table 3 that the C_{ad} values for **DPP1**–**3** are decreased considerably by the addition of CDCA irrespective of the obvious increase of J_{sc}. The observed increase of J_{sc} accompanied by the decrease of the adsorbed amount of dye demonstrates that CDCA acts effectively as co-adsorbate so as to suppress aggregation of dye molecules on TiO_2 responsible for the deactivation of photoexcited dyes. On the contrary, this implies that relatively small IPCE values below 50% observed with **DPP1**–**4**-based DSSCs without CDCA shown in Fig. 7(a)) are due, mostly, to the

Table 3
Photovoltaic parameters of DSSCs based on **DPP1**–**4**, **PE4T**, and **MK-2**.

Dye	[CDCA]/[dye][a]	[TBP]/M[b]	C_{ad}/cm^{-2}	J_{sc}/mA cm^{-2}	V_{oc}/V	*FF*	η (%)
DPP1	0	0	6.7×10^{13}	5.4	0.36	0.54	1.1
	1000	0	2.9×10^{13}	8.8	0.41	0.57	2.1
	0	0.5	6.7×10^{13}	0.7	0.48	0.61	0.2
	1000	0.5	2.9×10^{13}	0.9	0.52	0.66	0.3
DPP2	0	0	6.1×10^{13}	6.2	0.41	0.55	1.4
	200	0	2.9×10^{13}	9.0	0.43	0.54	2.1
DPP3	0	0	5.0×10^{13}	7.8	0.42	0.54	1.8
	20	0	3.3×10^{13}	8.9	0.44	0.52	2.0
DPP4	0	0	–	9.2	0.45	0.52	2.2
	200	0	–	13.7	0.48	0.50	3.3
	0	0.5	–	0.8	0.52	0.62	0.8
	200	0.5	–	4.4	0.55	0.64	1.6
PE4T	0	0	–	3.3	0.37	0.52	0.6
MK-2[c]	0	0	–	13.7	0.60	0.42	3.4

[a] Molar ratio of CDCA/dye in the solution for (co)adsorption on TiO_2.
[b] Concentration of TBP in the electrolyte.
[c] Data were obtained from the DSSC prepared by authors themselves.

aggregation of dye molecules adsorbed on TiO_2 and the bulky alkyl chains in **DPP1**–**4** do not serve necessarily well as units capable of hindering the dye aggregation. The V_{oc} values for **DPP1**–**4** were increased slightly when CDCA was added into the electrolyte: 0.36–0.41 V for **DPP1**, 0.41–0.43 V for **DPP2**, 0.42–0.44 V for **DPP3**, and 0.45–0.48 V for **DPP4**. However, they are still as small as or below 500 mV compared with those of DSSCs sensitized by other organic dyes [7,9,10]. The small V_{oc} values are likely to be accounted for in terms of the large dark currents, i.e., recombination of electrons injected from excited dyes to the conduction band of TiO_2 with the reducible species, I_3^- ions, in the electrolyte. To suppress such undesirable recombination process, TBP is widely used as an additive in the electrolyte solution [53]. When the TBP-containing electrolyte was used for **DPP1**-DSSC, V_{oc} and *FF* were improved from 0.36 to 0.48 V and from 0.54 to 0.61, respectively, but J_{sc} was drastically reduced from 5.4 to 0.7 mA cm^{-2}. This is also the case for the electrolyte including both TBP and CDCA: the J_{sc} value, for example, decreased from 8.8 to 0.9 mA cm^{-2} for **DPP1** and from 13.7 to 4.4 mA cm^{-2} for **DPP4**, respectively, upon addition of TBP in the electrolyte containing CDCA. It is known that the addition of TBP into the electrolyte induces the negative shift of the E_{CB} of TiO_2 by adsorption of pyridyl group of TBP onto the TiO_2 surface [55]. As Fig. 5 shows, the LUMO levels of **DPP1**–**4** lie only 0.4–0.5 eV above the E_{CB} of TiO_2, which is close to the threshold energy difference for the efficient electron injection from the photoexcited dyes to TiO_2 in the DSSCs without CDCA and TBP [2,12,56,57]. Therefore, when the E_{CB} of TiO_2 is shifted upwards by the addition of TBP, the electron injection probability may be greatly reduced because of the smaller energy difference and thus the J_{sc} may be decreased as shown in Table 3.

Finally, when the DSSC was fabricated with one of the panchromatic dyes developed here (**DPP4**) and CDCA as co-adsorbate, the **DPP4**-DSSC exhibited J_{sc} of 13.7 mA cm^{-2}, V_{oc} of 0.48 V, *FF* of 0.50, and thus the highest η of 3.3% among those for the DSSCs prepared in this study. This η value of 3.3% is apparently low, but it is comparable to 3.4% for the DSSC prepared by ourselves using **MK-2**, which is well-known as an excellent organic dye (Table 3). It indicates that **DPP4** will be a good candidate of dyes for the high-performance DSSC after the optimization of the cell fabrication technique.

4. Conclusion

We have designed and synthesized novel D-A-π-A dyes (**DPP1**–**4**), which have an electron-accepting DPP unit inserted in the EDOT-containing quaterthiophene π-linker. It was found that the introduction of the DPP unit induced a red-shift of absorption bands of the photosensitizing dyes. Accordingly, the photoactive regions of the DSSCs based on **DPP1**–**4** were extended far beyond 800 nm with extremely broad peaks centered at around 600 nm, although the very strong electron-withdrawing property of the DPP unit lowered the LUMO levels of these dyes. Substitution of a thiophene ring with a benzene ring in π-linker between DPP and CA units in **DPP4** caused an upward shift of the LUMO level, which enhanced injection probabilities of electrons from dye to TiO_2, resulting in the improvement of J_{sc} and η for **DPP4**-DSSC.

Acknowledgements

The authors are grateful to Drs. Tomoko Amimoto and Daisuke Kajiya, the Natural Science Center for Basic Research and Development (N-BARD), Hiroshima University for the measurement of mass spectroscopy.

Appendix A. Supplementary data

Supplementary data related to this article can be found at http://dx.doi.org/10.1016/j.orgel.2016.07.022.

References

[1] B. O'Regan, M. Grätzel, A low-cost, high-efficiency solar cell based on dye-sensitized colloidal TiO_2 films, Nature 353 (1991) 737–740.
[2] A. Hagfeldt, M. Grätzel, Light-induced redox reactions in nanocrystalline systems, Chem. Rev. 95 (1995) 49–68.
[3] A. Hagfeldt, G. Boschloo, L. Sun, L. Kloo, H. Pettersson, Dye-sensitized solar cells, Chem. Rev. 110 (2010) 6595–9993.
[4] Y.-S. Yen, H.-H. Chou, Y.-C. Chen, C.-Y. Hsu, J.T. Lin, Recent developments in molecule-based organic materials for dye-sensitized solar cells, J. Mater. Chem. 22 (2012) 8734–8747.
[5] S. Zhang, X. Yang, Y. Numata, L. Han, Highly efficient dye-sensitized solar cells: progress and future challenges, Energy Environ. Sci. 6 (2013) 1443–1464.
[6] Y. Chi, K.-L. Wu, T.-C. Wei, Ruthenium and Osmium complexes that bear functional azolate chelates for dye-sensitized solar cells, Chem. Asian. J. 10 (2015) 1098–1115.
[7] Y. Ooyama, Y. Harima, Molecular designs and syntheses of organic dyes for dye-sensitized solar cells, Eur. J. Org. Chem. 2009 (2009) 2903–2934.
[8] Y. Ooyama, Y. Harima, Photophysical and electrochemical properties, and molecular structures of organic dyes for dye-sensitized solar cells, ChemPhysChem 13 (2012) 4032–4080.
[9] Y. Wu, W. Zhu, Organic sensitizers from D-π-A to D-A-π-A: effect of the internal electron-withdrawing units on molecular absorption, energy levels and photovoltaic performances, Chem. Soc. Rev. 42 (2013) 2039–2058.
[10] M. Liang, J. Chen, Arylamine organic dyes for dye-sensitized solar cells, Chem. Soc. Rev. 42 (2013) 3453–3488.
[11] N. Manfredi, B. Cecconi, A. Abbotto, Multi-branched multi-anchoring metal-

free dyes for dye-sensitized solar cells, Eur. J. Org. Chem. 2014 (2014) 7069–7086.
[12] S. Qu, W. Wu, J. Hua, C. Kong, Y. Long, H. Tian, New diketopyrrolopyrrole (DPP) dyes for efficient dye-sensitized solar cells, J. Phys. Chem. C 114 (2010) 1343–1349.
[13] Y. Wu, W. Zhu, Organic sensitizers from D-π-A to D-A-π-A: effect of the internal electron-withdrawing units on molecular absorption, energy levels and photovoltaic performances, Chem. Soc. Rev. 42 (2013) 2039–2058.
[14] Y. Wu, W.-H. Zhu, S.M. Zakeeruddin, M. Grätzel, Insight into D-A-π-A structured sensitizers: a promising route to highly efficient and stable dye-sensitized solar cells, ACS Appl. Mater. Int. 7 (2015) 9307–9318.
[15] S. Qu, H. Tian, Diketopyrrolopyrrole (DPP)-based materials for organic photovoltaics, Chem. Commun. 48 (2012) 3039–3051.
[16] M. Kaur, D.H. Choi, Diketopyrrolopyrrole: brilliant red pigment dye-based fluorescent probes and their applications, Chem. Soc. Rev. 44 (2015) 58–77.
[17] W. Li, K.H. Hendriks, M.M. Wienk, R.A.J. Janssen, Diketopyrrolopyrrole polymers for organic solar cells, Acc. Chem. Res. 49 (2016) 78–85.
[18] F. Guo, S. Qu, W. Wu, J. Li, W. Ying, J. Hua, Synthesis and photovoltaic performance of new diketopyrrolopyrrole (DPP) dyes for dye-sensitized solar cells, Synth. Met. 160 (2010) 1767–1773.
[19] S. Qu, B. Wang, F. Guo, J. Li, W. Wu, C. Kong, Y. Long, J. Hua, New diketopyrrolo-pyrrole (DPP) sensitizer containing a furan moiety for efficient and stable dye-sensitized solar cells, Dyes Pigments 92 (2012) 1384–1393.
[20] J. Warnan, L. Favereau, Y. Pellegrin, E. Blart, D. Jacquemin, F. Odobel, A compact diketopyrrolopyrrole dye as efficient sensitizer in titanium dioxide dye-sensitized solar cells, J. Photochem. Photobiol. A Chem. 226 (2011) 9–15.
[21] S. Qu, C. Qin, A. Islam, Y. Wu, W. Zhu, J. Hua, H. Tian, L. Han, A novel D-A-π-A organic sensitizer containing a diketopyrrolopyrrole unit with a branched alkyl chain for highly efficient and stable dye-sensitized solar cells, Chem. Commun. 48 (2012) 6972–6974.
[22] S. Qu, C. Qin, A. Islam, J. Hua, H. Chen, H. Tian, L. Han, Tuning the electrical and optical properties of diketopyrrolopyrrole complexes for panchromatic dye-sensitized solar cells, Chem. Asian J. 7 (2012) 2895–2903.
[23] T.W. Holcombe, J.-H. Yum, J. Yoon, P. Gao, M. Marszalek, D. Di Censo, K. Rakstys, Md K. Nazeeruddin, M. Graetzel, A structural study of DPP-based sensitizers for DSC applications, Chem. Commun. 48 (2012) 10724–10726.
[24] J.-H. Yum, T.W. Holcombe, Y. Kim, J. Yoon, K. Rakstys, M.K. Nazeeruddin, M. Grätzel, Towards high-performance DPP-based sensitizers for DSC applications, Chem. Commun. 48 (2012) 10727–10729.
[25] F. Zhang, K.-J. Jiang, J.-H. Huang, C.-C. Yu, S.-G. Li, M.-G. Chen, L.-M. Yan, Y.-L. Song, A novel compact DPP dye with enhanced light harvesting and charge transfer properties for highly efficient DSCs, J. Mater. Chem. A 1 (2013) 4858–4863.
[26] L. Favereau, J. Warnan, Y. Pellegrin, E. Blart, M. Boujtita, D. Jacquemin, F. Odobel, Diketopyrrolopyrrole derivatives for efficient NiO-based dye-sensitized solar cells, Chem. Commun. 49 (2013) 8018–8020.
[27] T.W. Holcombe, J.-H. Yum, Y. Kim, K. Rakstys, M. Grätzel, Diketopyrrolo-pyrrole-based sensitizers for dyesensitized solar cell applications: anchor engineering, J. Mater. Chem. A 1 (2013) 13978–13983.
[28] J.-H. Huang, K.-J. Jiang, F. Zhang, W. Wu, S.-G. Li, L.-M. Yang, Y.-L. Song, Engineering diketopyrrolopyrrole sensitizers for highly efficient dye-sensitized solar cells: enhanced light harvesting and intramolecular charge transfer, RSC Adv. 4 (2014) 16905–16912.
[29] S.-S. Li, K.-J. Jiang, F. Zhang, J.-H. Huang, S.-G. Li, M.-G. Chen, L.-M. Yang, Y.-L. Song, New diketopyrrolopyrrole-based organic dyes for highly efficient dye-sensitized solar cells, Org. Electr. 15 (2014) 1579–1585.
[30] P. Ganesan, A. Yella, T.W. Holcombe, P. Gao, R. Rajalingam, S.A. Al-Muhtaseb, M. Grätzel, M.K. Nazeeruddin, Unravel the impact of anchoring groups on the photovoltaic performances of diketopyrrolopyrrole sensitizers for dye-sensitized solar cells, ACS Sus. Chem. Eng. 3 (2015) 2389–2396.
[31] I. Imae, K. Korai, Y. Ooyama, K. Komaguchi, Y. Harima, Synthesis of novel dyes having EDOT-containing oligothiophenes as π-linker for panchromatic dye-sensitized solar cells, Synth. Met. 207 (2015) 65–71.
[32] I. Imae, T. Koshima, K. Korai, Y. Ooyama, K. Komaguchi, Y. Harima, Enhanced photovoltaic performances of panchromatic EDOT-containing dye by introducing bulky dialkylfluorene units in donor moiety, Dyes Pigments 132 (2016) 262–269.
[33] I. Imae, S. Imabayashi, K. Korai, T. Mashima, Y. Ooyama, K. Komaguchi, Y. Harima, Electrosynthesis and charge-transport properties of poly(3′,4′-ethylenedioxy-2,2′:5′,2″-terthiophene), Mater. Chem. Phys. 131 (2012) 752–756.
[34] I. Imae, S. Imabayashi, K. Komaguchi, Z. Tan, Y. Ooyama, Y. Harima, Synthesis and electrical properties of novel oligothiophenes partially containing 3,4-ethylenedioxythiophenes, RSC Adv. 4 (2014) 2501–2508.
[35] I. Imae, H. Sagawa, T. Mashima, K. Komaguchi, Y. Ooyama, Y. Harima, Synthesis of soluble polythiophene partially containing 3,4-ethylenedioxythiophene and 3-hexylthiophene by polycondensation, Open J. Polym. Chem. 4 (2014) 83–93.
[36] I. Imae, T. Mashima, H. Sagawa, K. Komaguchi, Y. Ooyama, Y. Harima, In situ conductivity measurements of polythiophene partially containing 3,4-ethylenedioxythiophene and 3-hexylthiophene, J. Solid State Electrochem. 19 (2015) 71–76.
[37] I. Imae, R. Ogino, Y. Tsuboi, T. Goto, K. Komaguchi, Y. Harima, Synthesis of EDOT-containing polythiophenes and their properties in relation to the composition ratio of EDOT, RSC Adv. 5 (2015) 84694–84702.
[38] N. Koumura, Z.-S. Wang, S. Mori, M. Miyashita, E. Suzuki, K. Hara, Alkyl-functionalized organic dyes for efficient molecular photovoltaics, J. Am. Chem. Soc. 128 (2006) 14256–14257.
[39] R. Pudzich, J. Salbeck, Synthesis and characterization of new oxadiazoleamine based spiro-linked fluorescence dyes, Synth. Met. 138 (2003) 21–31.
[40] K.S.V. Gupta, S.P. Singh, A. Islam, L. Han, M. Chandrasekharam, Simple fluorene based triarylamine metal-free organic sensitizers, Electrochim. Acta 174 (2015) 581–587.
[41] A.B. Tamayo, M. Tantiwiwat, B. Walker, T.-Q. Nguyen, Design, synthesis, and self-assembly of oligothiophene derivatives with a diketopyrrolopyrrole core, J. Phys. Chem. C 112 (2008) 15543–15552.
[42] V.V. Pavlishchuk, A.W. Addison, Conversion constants for redox potentials measured versus different reference electrodes in acetonitrile solutions at 25 °C, Inorg. Chim. Acta 298 (2000) 97–102.
[43] Gaussian 09, Revision D.01, M. J. Frisch, G. W. Trucks, H. B. Schlegel, G. E. Scuseria, M. A. Robb, J. R. Cheeseman, G. Scalmani, V. Barone, B. Mennucci, G. A. Petersson, H. Nakatsuji, M. Caricato, X. Li, H. P. Hratchian, A. F. Izmaylov, J. Bloino, G. Zheng, J. L. Sonnenberg, M. Hada, M. Ehara, K. Toyota, R. Fukuda, J. Hasegawa, M. Ishida, T. Nakajima, Y. Honda, O. Kitao, H. Nakai, T. Vreven, J. A. Montgomery, Jr., J. E. Peralta, F. Ogliaro, M. Bearpark, J. J. Heyd, E. Brothers, K. N. Kudin, V. N. Staroverov, R. Kobayashi, J. Normand, K. Raghavachari, A. Rendell, J. C. Burant, S. S. Iyengar, J. Tomasi, M. Cossi, N. Rega, J. M. Millam, M. Klene, J. E. Knox, J. B. Cross, V. Bakken, C. Adamo, J. Jaramillo, R. Gomperts, R. E. Stratmann, O. Yazyev, A. J. Austin, R. Cammi, C. Pomelli, J. W. Ochterski, R. L. Martin, K. Morokuma, V. G. Zakrzewski, G. A. Voth, P. Salvador, J. J. Dannenberg, S. Dapprich, A. D. Daniels, Ö. Farkas, J. B. Foresman, J. V. Ortiz, J. Cioslowski, and D. J. Fox, Gaussian, Inc, Wallingford CT, 2009.
[44] Y. Harima, T. Fujita, Y. Kano, I. Imae, K. Komaguchi, Y. Ooyama, J. Ohshita, Lewis-acid sites of TiO_2 surface for adsorption of organic dye having pyridyl group as anchoring unit, J. Phys. Chem. C 117 (2013) 16364–16370.
[45] A. Fillinger, B.A. Parkinson, The adsorption behavior of a ruthenium-based sensitizing dye to nanocrystalline TiO_2 coverage effects on the external and internal sensitization quantum yields, J. Electrochem. Soc. 146 (1999) 4559–4564.
[46] M.K. Nazeeruddin, P. Péchy, T. Renouard, S.M. Zakeeruddin, R. Humphry-Baker, P. Comte, P. Liska, L. Cevey, E. Costa, V. Shklover, L. Spiccia, G.B. Deacon, C.A. Bignozzi, M. Grätzel, Engineering of efficient panchromatic sensitizers for nanocrystalline TiO_2-based solar cells, J. Am. Chem. Soc. 123 (2001) 1613–1624.
[47] S. Ushiroda, N. Ruzycki, Y. Lu, M.T. Spitler, B.A. Parkinson, Dye sensitization of the anatase (101) crystal surface by a series of dicarboxylated thiacyanine dyes, J. Am. Chem. Soc. 127 (2005) 5158–5168.
[48] K.-J. Hwang, W.-G. Shim, S.-H. Jung, S.-J. Yoo, J.-W. Lee, Analysis of adsorption properties of N719 dye molecules on nanoporous TiO_2 surface for dye-sensitized solar cell, Appl. Sur. Sci. 256 (2010) 5428–5433.
[49] C.Y. Lee, C. She, N.C. Jeong, J.T. Hupp, Porphyrin sensitized solar cells: TiO_2 sensitization with a π-extended porphyrin possessing two anchoring groups, Chem. Commun. 46 (2010) 6090–6092.
[50] Y. Sakuragi, X.-F. Wang, H. Miura, M. Matsui, T. Yoshida, Aggregation of indoline dyes as sensitizers for ZnO solar cells, J. Photochem. Photobiol. A Chem. 216 (2010) 1–7.
[51] Y. Hara, M.I. Tejedor-Tejedor, K. Lara, D. Lubin, L.J. Brzozowski, D.J. Severseike, M.A. Anderson, Importance of adsorption isotherms in defining performance of dye-sensitized solar cells fabricated from photoelectrodes composed of ZnO nanopowders and nanorods, Electrochim. Acta 56 (2011) 8873–8879.
[52] A. Kay, M. Grätzel, Artificial photosynthesis. 1. Photosensitization of TiO_2 solar cells with chlorophyll derivatives and related natural porphyrins, J. Phys. Chem. 97 (1993) 6272–6277.
[53] M.K. Nazeeruddin, A. Kay, I. Rodicio, R. Humpbry-Baker, E. Miiller, P. Liska, N. Vlachopoulos, M. Grätzel, Conversion of light to electricity by *cis*-X_2bis(2,2′-bipyridyl-4,4′-dicarboxylate)ruthenium (II) charge-transfer sensitizers (X = C1-, Br-, I-, CN-, and SCN-) on nanocrystalline TiO2 electrodes, J. Am. Chem. Soc. 115 (1993) 6382–6390.
[54] K. Hara, Y. Dan-oh, C. Kasada, Y. Ohga, A. Shinpo, S. Suga, K. Sayama, H. Arakawa, Effect of additives on the photovoltaic performance of coumarin-dye-sensitized nanocrystalline TiO_2 solar cells, Langmuir 20 (2004) 4205–4210.
[55] H. Kusama, H. Orita, H. Sugihara, TiO_2 band shift by nitrogen-containing heterocycles in dye-sensitized solar cells: a periodic density functional theory study, Langmuir 24 (2008) 4411–4419.
[56] S.S. Pandey, T. Inoue, N. Fujikawa, Y. Tamaguchi, S. Hayase, Substituent effect in direct ring functionalized squaraine dyes on near infra-red sensitization of nanocrystalline TiO_2 for molecular photovoltaics, J. Photochem. Photobiol. A Chem. 214 (2010) 269–275.
[57] D. Joly, L. Pellejà, S. Narbey, F. Oswald, T. Meyer, Y. Kervella, P. Maldivi, J.N. Clifford, E. Palomares, R. Demadrille, Metal-free organic sensitizers with narrow absorption in the visible for solar cells exceeding 10% efficiency, Energy Environ. Sci. 8 (2015) 2010–2018.